Proceedings of the
International Conference on Mechanical Engineering 2011
(ICME2011) 18-20 December 2011, Dhaka, Bangladesh

ICME11-FL-030

NATURAL CONVECTION OF AIR IN TILTED SQUARE CAVITIES WITH DIFFERENTIALLY HEATED OPPOSITE WALLS

Kunja Bihari Sahu[1], Manas Ranjan Padhi[2], Prakash Ghose[1] and D K Ray[2]

[1] KIIT University, Bhubaneswar-751024, Odisha, India
[2] C V Raman College of Engineering, Bhubaneswar, Odisha, India

ABSTRACT

Natural convection in air-filled, inclined square enclosures with two adjacent walls heated and the other two walls cooled is numerically studied. The governing equations are discretised with finite elements using Galerkin's method. Simulations are performed for different values of Rayleigh numbers (*Ra*) in the range of $10^3 \le Ra \le 10^5$, and of the inclination angle (γ) of the enclosure in the range of $0° \le \gamma \le 360°$. The influence of *Ra* and γ on the temperature distribution, flow pattern, and heat flux are discussed.

Keywords: FEM, Galerkin Method, Inclined Square Enclosure, Rayleigh Number.

1. INTRODUCTION

Most of the studies performed on natural convection heat transfer within enclosed spaces are related to buoyancy induced by imposing a heat flux or a temperature difference either horizontally or vertically from below in examining conventional convection or thermal instabilities respectively. Detailed reviews on this topic are given by Ostrach, 1988 [1] and Bejan, 2004 [2]. Several works have also been done where the assigned thermal gradient is neither simply horizontal nor vertical. Ganzarolli and Milanez, 1995 [3] have studied on rectangular cavities heated from below and cooled along both sides. Aydin et al., 1995 [4] have investigated the effects of heating from one side and cooled from top of a rectangular cavity. In the above-cited works, untilted cavity has been considered. Inclination effects may be of interest in many science and engineering applications. The buoyancy force components change with orientation, which may cause transition between different flow patterns and may change heat transfer rates considerably. Ciafrini et al., 2005 [5] studied the thermal behaviour of inclined square cavity with two adjacent sides heated (both at same temperature), and the other two adjacent sides cooled (both at same temperature). Through heat transfer measurements, Hollands and Konicek, 1973 [6] confirmed a changeover angle, at which it was presumably caused by a transition between two different flow patterns. Arnold et al., 1976 [7] also demonstrated the existence of this changeover phenomenon. Soong et al., 1996 [8] have studied numerically the mode transition of natural convection in inclined cavities. Catton et al., 1974 [9], by using Galerkin method, solved two-dimensional flow and temperature fields in inclined cavities of various aspect ratios. However, only limited information about the flow pattern is provided. In the present work, the natural convection in air within inclined square enclosure has been considered. Two adjacent walls of the enclosure are heated whereas the other two walls are cooled isothermally. The mass and momentum conservation equations are in stream function-vorticity form. These equations along with energy conservation equations are discretised using finite element method. The influences of Rayleigh number and inclination angle on the temperature distribution, flow pattern, and heat flux have been discussed.

2. ANALYSIS

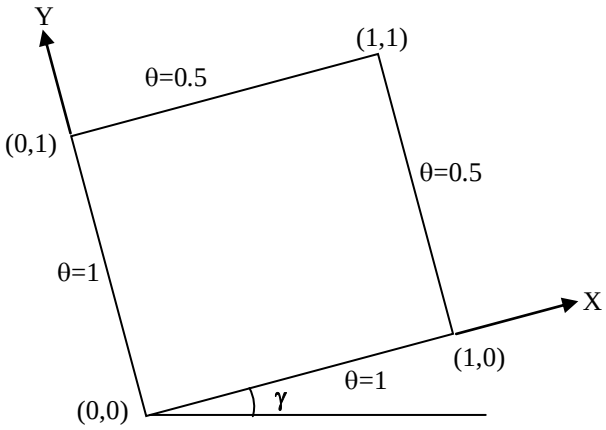

Fig 1. Computational domain and coordinate system.

Consider an air-filled square cavity of side L. Two adjacent walls are maintained at temperature T_H, while the two opposite walls cooled to temperature T_C. The

corresponding non-dimensional temperatures are θ_H=1 and θ_C=0.5 respectively. The computational domain with coordinate system is depicted in Fig. 1. 2 -D laminar flow, with constant fluid properties and negligible viscous dissipation, is considered. No slip condition is assumed at four walls of the cavity and Boussinesq approximation is employed for gravity terms in the momentum conservation equation. The governing Navier-Stoke's equations in stream function-vorticity form are

$$\nabla^2\psi = -\omega \tag{1}$$

$$u\frac{\partial\omega}{\partial x} + v\frac{\partial\omega}{\partial y} = \nu\nabla^2\omega + g\beta\frac{\partial T}{\partial x}\cos\gamma - g\beta\frac{\partial T}{\partial y}\sin\gamma \tag{2}$$

For 2-D steady state, constant fluid properties without internal heat generation, and negligible viscous dissipation, the energy conservation equation can be expressed as,

$$u\frac{\partial T}{\partial x} + v\frac{\partial T}{\partial y} = \alpha\left(\frac{\partial^2 T}{\partial x^2} + \frac{\partial^2 T}{\partial y^2}\right) \tag{3}$$

The boundary conditions are

$$\psi = 0, \quad \text{at all walls} \tag{4}$$

$$\omega_{i,J} = \frac{-2\left(\psi_{i,J+1} - \psi_{i,J}\right)}{(\Delta y)^2} \tag{5}$$

(where, i , J represents a point on the wall, and i, J+1 represents a point on an adjacent layer at a distance Δy from the wall [2])

$$T = T_H, \quad at \quad x = 0, and \quad at\ y = 0 \tag{6}$$

$$T = T_C, \quad at \quad x = L, and \quad at\ y = L \tag{7}$$

The following parameters are used for expressing above governing equations in dimensionless form.

$$X = \frac{x}{L},\ Y = \frac{y}{L},\ \psi^* = \frac{\psi}{\alpha},\ \omega^* = \frac{\omega}{(\alpha/L^2)},$$

$$u^* = \frac{u}{(\alpha/L)},\ v^* = \frac{v}{(\alpha/L)},\ \theta = \frac{T}{T_H} \tag{8}$$

Using the above dimensionless quantities, the governing equations can be expressed as,

$$\nabla^2\psi^* = -\omega^* \tag{9}$$

$$u^*\frac{\partial\omega^*}{\partial X} + v^*\frac{\partial\omega^*}{\partial Y} =$$

$$\Pr\nabla^2\omega^* + \Pr Ra\cos\gamma\frac{\partial\theta}{\partial X} - \Pr Ra\sin\gamma\frac{\partial\theta}{\partial Y} \tag{10}$$

$$u^*\frac{\partial\theta}{\partial X} + v^*\frac{\partial\theta}{\partial Y} = \nabla^2\theta \tag{11}$$

and the boundary conditions are

$$\psi^* = 0\ , \quad \text{at all walls} \tag{12}$$

$$\omega^*_{i,J} = \frac{-2(\psi^*_{i,J+1} - \psi^*_{i,J})}{(\Delta Y)^2} \tag{13}$$

$$\theta = 1, \quad at \quad X = 0; \quad and\ at\ Y = 0 \tag{14}$$

$$\theta = \frac{T_C}{T_H}, \quad at \quad X = 1; \quad and\ at\ Y = 0 \tag{15}$$

3. NUMERICAL PROCEDURE

The computational domain is represented by 21×21 nodes and 800 linear triangular elements. All the governing equations for mass, momentum and energy conservation are numerically discretized in the computational domain using above-mentioned triangular elements. The triangular elements taken here are linear isoparametric and all the variables like ψ*, ω*, u*, v* and θ at any point within the element are expressed in terms of the nodal values by using the linear shape functions. The same shape functions are used to get the coordinates at any point within the element in terms of the nodal coordinates. The shape functions are used to seek an approximate solution which introduces an error called the residual. The Galerkin's method is presented as one of the weighted residual methods where the residual is set to zero relative to a weighting function. First, the element equations are developed using Galerkin's method and then assembled in order to get equations for the whole computational domain. The isothermal boundary conditions for all the walls are imposed, which modifies both the conductivity matrix and heat rate vector appropriately. The governing equations for momentum (Eqn. 10) and energy conservation (Eqn. 11) are coupled through source terms. Therefore the solution of the above equations can only be obtained through iteration. The flow chart of numerical procedure has been outlined in Fig. 2. During the numerical investigation, it is experienced by the authors that, under-relaxation of momentum equation and energy equation is required for obtaining the convergence.

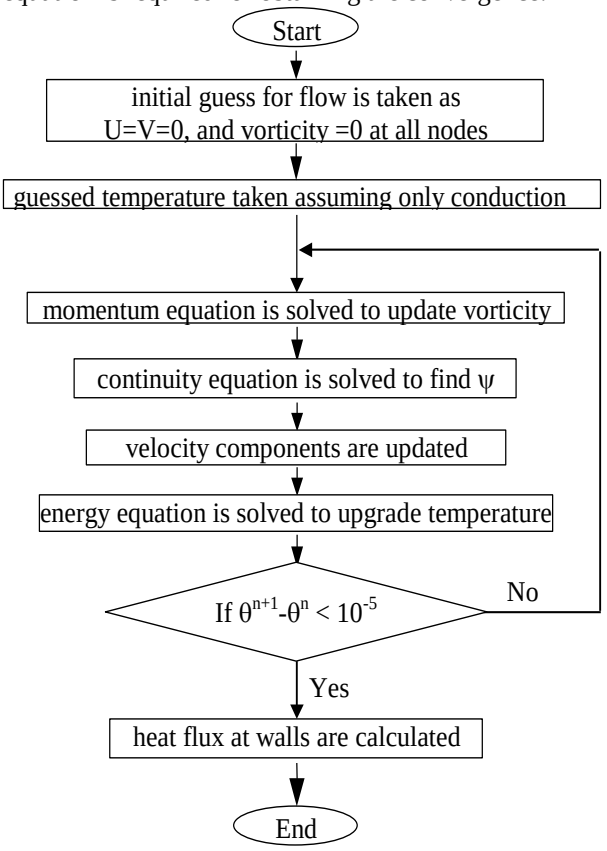

Fig 2. Flow chart for solving the problem

Table 1: Comparison of present prediction with benchmark solution

Quantities	Benchmark	Present	Deviation
	$Ra=10^3$		
u_{max}	3.649	3.632	-0.46%
(x,y)	(0.5, 0.813)	(0.5,0.8)	
v_{max}	3.697	3.657	-1.08%
(x,y)	(0.181, 0.5)	(0.15,0.5)	
Nu	1.118	1.115	-0.29%
Nu_{max}	1.505	1.499	-0.38%
Nu_{min}	0.692	0.692	0.0%
	$Ra=10^4$		
u_{max}	16.178	16.506	2.02%
(x,y)	(0.5, 0.823)	(0.5,0.85)	
v_{max}	19.617	19.330	-1.46%
(x,y)	(0.119, 0.5)	(0.15,0.5)	
Nu	2.243	2.250	0.33%
Nu_{max}	3.528	3.567	1.10%
Nu_{min}	0.586	0.576	1.66%

The code used here was validated against the benchmark solution of G. de Vahl Davis, 1983 [10]. The natural convection of air in a square cavity with the boundary conditions prescribed in the benchmark solution is solved for $Ra=10^3$ and 10^4. The present predictions and the corresponding benchmark solutions are depicted in Table 1. The accuracy of the solution, which has been tested from the energy balance for the cavity and the validation stated above, does not encourage the authors to work with very fine mesh size at the cost of computational time.

Once the convergence is reached, the Nusselt numbers of the hot wall and cold wall are calculated using the following expressions:

$$Nu_{HX} = \frac{Q_{HX}}{k(T_H - T_C)} = -\int_0^1 \left.\frac{\partial\theta}{\partial Y}\right|_{Y=0} dX \qquad (9)$$

$$Nu_{HY} = \frac{Q_{HY}}{k(T_H - T_C)} = -\int_0^1 \left.\frac{\partial\theta}{\partial X}\right|_{X=0} dY \qquad (10)$$

$$Nu_{CX} = \frac{Q_{CX}}{k(T_C - T_H)} = +\int_0^1 \left.\frac{\partial\theta}{\partial Y}\right|_{Y=1} dX \qquad (11)$$

$$Nu_{CY} = \frac{Q_{CY}}{k(T_C - T_H)} = +\int_0^1 \left.\frac{\partial\theta}{\partial X}\right|_{X=1} dY \qquad (12)$$

It may be noted that at the steady-state condition, the Nusselt numbers Nu_{HY} and Nu_{CY} (for the hot and cold walls along y-direction respectively) are taken as the average Nusselt number Nu_x across the cavity along the x-direction, and that the Nusselt numbers Nu_{HX} and Nu_{CX} (for the hot and cold walls along x-direction respectively) are considered as the average Nusselt number Nu_y across the cavity along the y-direction.

$Nu_x = Nu_{HY} = Nu_{CY}$

$Nu_y = Nu_{HX} = Nu_{CX}$

In addition, also the average Nusselt number Nu of the whole enclosure is calculated as,

$Nu = 0.5(Nu_x + Nu_y)$

3. RESULTS AND DISCUSSION

Numerical simulations are performed for Pr=0.71, which corresponds to air, and for different values of Rayleigh number in the range of $10^3 \le Ra \le 10^5$, and of the inclination angle of the cavity in the range of $0° \le \gamma \le 360°$. In the figures for isotherm and velocity vector plots, the hot wall along x-axis is represented as 'HX' and that along y-axis is represented as 'H' to make clear the walls at different inclined positions. The contour lines of isotherm plots correspond to equally spaced values of θ in the range between 1 and 0.5. The velocity vectors are plotted with a fixed scale for comparison of magnitude of the velocities. As far as heat transfer rates are concerned, the variation of average Nusselt number versus inclination angle is reported for different Rayleigh numbers. The results may be analysed and discussed as follows.

3.1 Effect Of Rayleigh Number

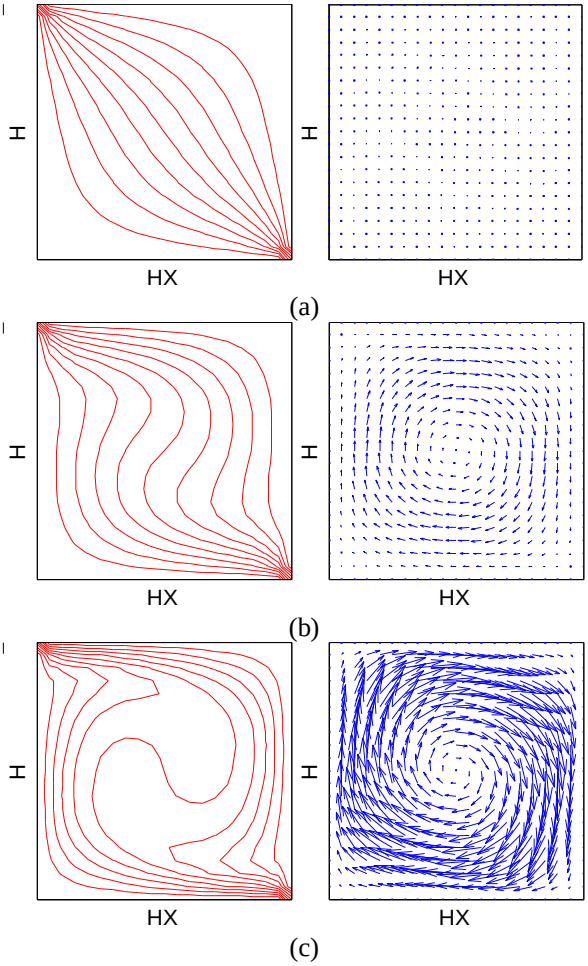

Fig 3. Isotherms and velocity vectors for (a) $Ra=10^3$, (b) $Ra=10^4$, (c) $Ra=10^5$ (at $\gamma=0°$)

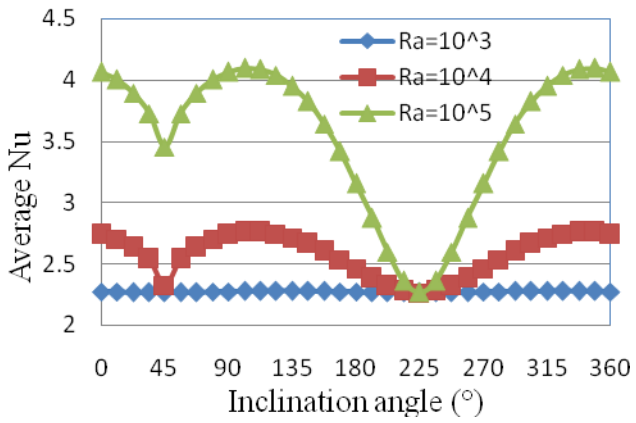

Fig 4. Average Nusselt number (Nu) vrs Inclination angles (γ) (Ra=10^3, Ra=10^4, Ra=10^5)

At γ=0°, for lower value of Rayleigh number, say 10^3, the curvature of the isotherms are not large as shown in Fig. 3(a), which implies less effect of convection. Keeping hot wall temperature constant, increase in Rayleigh number implies increased size of the enclosure, which strengthens buoyancy effect. As Rayleigh number increases, the clockwise motion increases and the curvature of the isotherms increase as seen from the Figs. 3(b) and 3(c). The motion of the fluid is almost uniform throughout the enclosure except at the center and all the corners and the velocity is increased as *Ra* is increased. As motion of the fluid increases, more amount of heat is taken away from the hot wall to the cold wall. So for any inclined position, the heat transfer rate increases as Rayleigh number increases (Fig. 4).

3.2 Effect Of Inclination Angle

3.2.1 Inclination angle in the range 0° ≤ γ ≤ 45°

As the inclination angle of the enclosure γ increases, the clockwise fluid motion progressively slows down. This is due to the increasing buoyant action driven by hot wall and cold wall in the x-direction, which would tend to impose an anticlockwise fluid circulation. The buoyant force is directed towards the core with increase in γ. The buoyancy force pushes the fluid near the walls towards the core. So the stagnant core gets motion and the motion in the core is more compared to that near the wall. The single-cell flow pattern gets more and more distorted, due to the progressive enlargement of the quasi-stagnant regions at the bottom and top corners of the enclosure (Fig. 5). As far as heat transfer rate is concerned, it is almost of pure conduction for Ra=10^3. For higher Rayleigh numbers, the heat transfer rate decreases continuously from 0° to 45° (Fig. 4). This is due to the fact that more fluid is circulated inside the core rather than near the wall. So less amount of fluid take part in carrying the heat from hot walls towards the cold walls.

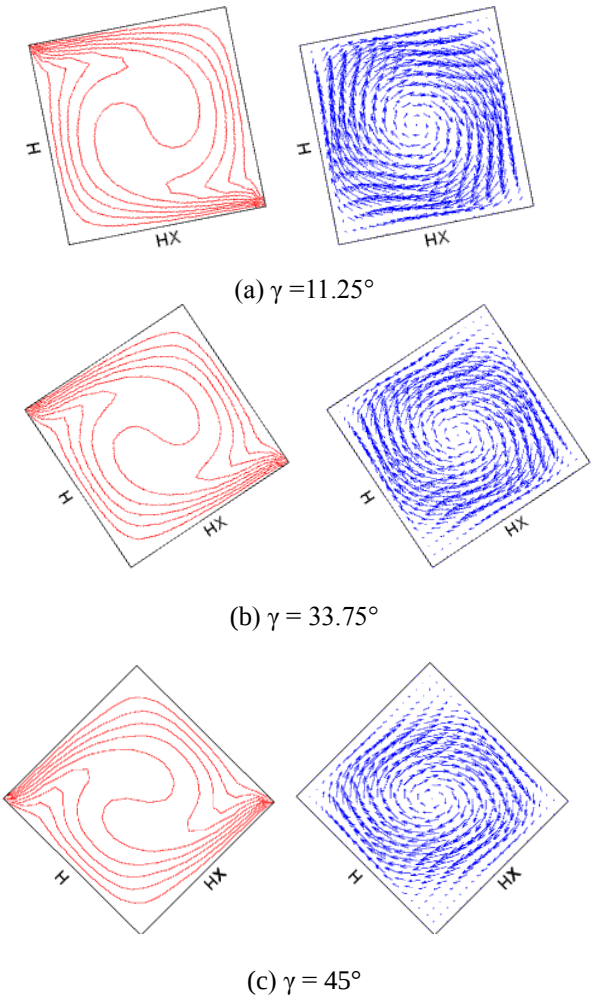

Fig 5. Isotherms and velocity vectors for Ra=10^5 (at γ =11.25°, 33.75°, 45°)

3.2.2 Inclination angle in the range 45°<γ≤90°

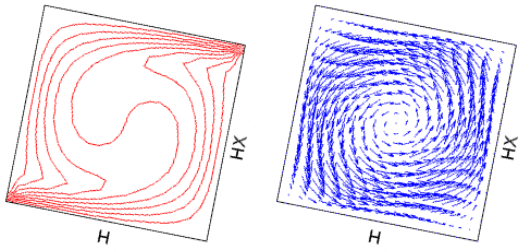

Fig. 6 Isotherms and velocity vectors for Ra=10^5 (at γ = 78.75°)

As γ is increased more than 45°, the isotherms and velocity vector plots at any inclination angle γ are same as those corresponding to the inclination angle (90°–γ), but the motion is anti-clockwise (Fig. 6). The average heat transfer rate is same as that for angle (90°–γ) (Fig. 4).

3.2.3 Inclination angle in the range 90°<γ≤180°

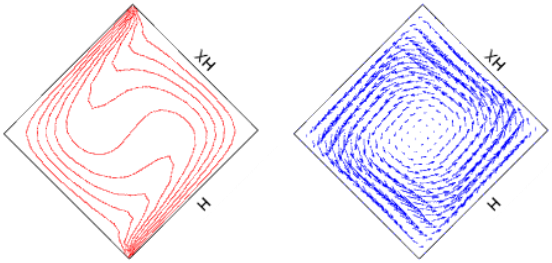

(a) γ =135°

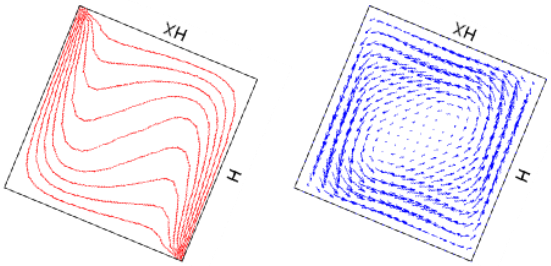

(b) γ = 157.5°

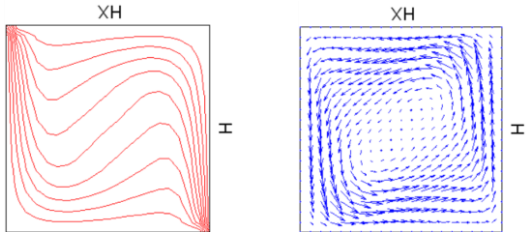

(c) γ==180°

Fig 7. Isotherms and velocity vectors for Ra=10^5 (at γ =135°, 157.5°, 180°)

As γ is increased beyond 90°, the buoyant action driven by the hot walls and cold walls along y-direction and that driven by the hot walls and cold walls along x-direction, are in the same direction, thus leading to a faster circulation of the fluid. At γ=135°, a typical boundary layer motion around a motionless core may be well distinguished Fig. 7(a). Also the isotherm pattern gives core stratification similar to that typical for vertical enclosures with differentially heated sidewalls. In contrast, as γ is further increased, the strength of the fluid circulation decreases as the thermal driving-force brought about by both hot wall & cold wall along x-direction progressively decreases (Fig. 7b).

At γ=180°, a pronounced fluid stratification, which derives from the over-stabilizing effect induced by the downward -imposed vertical temperature gradient, may be observed (Fig. 7c). As far as the heat transfer rates are concerned, it can be noticed that the Nusselt number Nu increases from 90° up to 135° and then decreases.

3.2.4 Inclination angle in the range 180°<γ≤225°

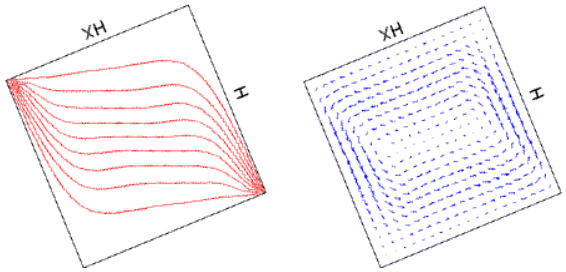

(a) γ = 202.5°

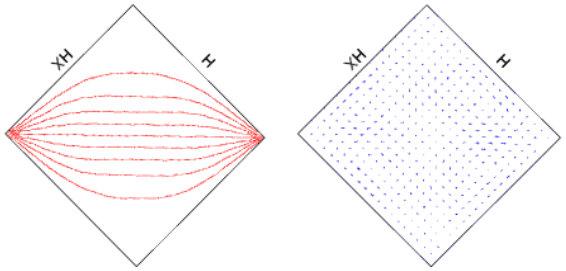

(b) γ = 225°

Fig 8. Isotherms and velocity vectors for Ra=10^5 (at γ = 202.5°, 225°)

As γ is increased from 180°, the thermal driving actions delivered by the two hot walls are in contrast with one another, thus tending to cancel each other out. The same consideration applies to the cold walls. So the motion of the fluid in the enclosure slows down, which can be seen from the Fig. 8. The isotherms are nearly straight, representing less convection. Due to slow down of fluid motion, the rate of heat transfer decreases (Fig. 4). At γ=225°, a practically motionless conductive field is observed (Fig. 8b).

It is interesting to note that at γ=225°, Nu reach the value typical of pure conduction which would derive from the solution of only the equation of energy.

3.2.5 Inclination angle in the range 225°<γ<360°

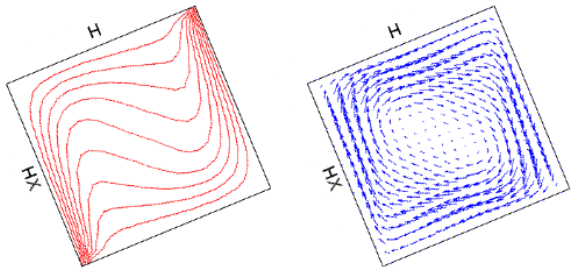

Fig 9. Isotherms and velocity vectors for Ra=10^5 (at γ = 292.5°)

As γ exceeds 225°, the isotherms and velocity vector plots at any inclination angle γ are same as those corresponding to the inclination angle (450° −γ), but the motion is clockwise (Fig. 9 and Fig. 7b). For this, the heat transfer rate is similar to that for the positions in the range 90°<γ<225° (Fig. 4).

4. CONCLUSIONS

Natural convection in air-filled, inclined square enclosures with two adjacent walls heated and the other two walls cooled is numerically studied. The following conclusions are made from the study.

- For a sufficiently wide range of γ around 135°, the overall heat transfer along x-direction across the enclosure is larger than that corresponding to normal case, i.e., γ =0°.
- For a sufficiently wide range of γ around 315°, the overall heat transfer along x-direction across the enclosure is larger than that corresponding to normal case, i.e., γ =0°.
- The overall heat transfer in the enclosure is almost same around 0° and 90° .The overall heat transfer is maximum slightly before 0° and slightly after 90° and both are of same magnitude.
- For γ=225°, the Nusselt number is same as that for pure conduction.
- All the observations noted above are not significant for Ra=10^3 as the convection effect is not prominent.

5. REFERENCES

1. Ostrach, S., "Natural convection in enclosures," J. Heat Transfer, Vol. 110, 1988, pp. 1175-1190.
2. Bejan, A., Convection Heat Transfer, 3rd ed., John Wiley & Sons, Inc., Hoboken, New Jersey, 2004, pp. 243-306.
3. Ganzarolli, M. M., Milanez, L. F., "Natural convection in rectangular enclosures heated from below and symmetrically cooled from the sides," Int. J. Heat Mass Transfer, Vol. 38, 1995, pp. 1063-1073.
4. Aydin, O., Unal, A., Ayhan, T., "Natural convection in rectangular enclosures heated from one side and cooled from the ceiling," Int. J. Heat Mass Transfer, Vol. 42, 1999, pp. 2345-2355.
5. Cianfrini, C., Corcione, M., Dell'Omo, P. P., "Natural convection in tilted square cavities with differentially heated opposite walls," Int. J. Thermal Sciences, Vol. 44, 2005, pp. 441-451.
6. Hollands, K. G. T., and Konicek, L., "Experimental study of the stability of differentially heated inclined air layers," lnt. J. Heat Mass Transfer, Vol. 16, 1973, pp. 1467-1476.
7. Arnold, J. N., Catton, I., and Edwards, D. K., "Experimental investigation of natural convection in inclined rectangular regions of differing aspect ratios," ASME J. Heat Transfer, Vol. 98, 1976, pp. 67-71.
8. Soong, C. Y., Tzeng, P. Y., Chiang, D. C., and Sheu, T. S., "Numerical study on mode-transition of natural convection in differentially heated inclined enclosures," Int. J. Heat Mass Transfer, Vol. 39, 1996, pp. 2869-2882.
9. Catton, I., Ayyaswammy, P. and Clever, R. M., "Natural convection flow in a finite, rectangular slot arbitrarily oriented with respect to the gravity vector," Int. J. Heat Mass Transfer, vol. 17, pp. 173-184, 1974.
10. Davis, G. de Vahl, "Natural convection of air in a square cavity: A benchmark numerical solution," Int. J. Numerical Methods Fluids, vol. 3, pp. 249-264, 1983.

6. NOMENCLATURE

Symbol	Meaning	Unit
g	Acceleration due to gravity	(m/s^2)
k	Thermal conductivity	(W/mK)
L	Length of each side of the cavity	(m)
Pr	Prandtl Number (dimensionless)	(--)
q	Heat flux	(W/m^2)
Q	Heat flux (dimensionless)	(--)
Ra	Rayleigh Number (dimensionless)	(--)
T	Temperature	(K)
u	Velocity component along x-direction	(m/s)
u*	Velocity component along x-direction (dimensionless)	(--)
v	Velocity component along y-direction	(m/s)
v*	Velocity component along y-direction (dimensionless)	(--)
x	Co-ordinate in x-direction	(m)
X	Co-ordinate in x-direction (dimensionless)	(--)
y	Co-ordinate in y-direction	(m)
Y	Co-ordinate in y-direction (dimensionless)	(--)
α	Thermal diffusivity	(m^2/s)
β	Volumetric co-efficient of thermal expansion	(K^{-1})
γ	Inclination angle of the cavity	(°)
ν	Kinematic viscosity	(m^2/s)
θ	Temperature (dimensionless)	(--)
ρ	Density	(kg/m^3)
ω	Vorticity	(s^{-1})
ω*	Vorticity (dimensionless)	(--)
ψ	Stream function	(m^2/s)
ψ*	Stream function (dimensionless)	(--)

Subscripts

c= Conduction
C=Cold wall
H= Hot wall

8. MAILING ADDRESS

Kunja Bihari Sahu
KIIT University,
Bhubaneswar-751024,
Odisha, India